

How “cold” are the stellar discs of superthin galaxies?

K.Aditya^{1*} and Arunima Banerjee^{2,†}

{1, 2} *Indian Institute of Science Education and Research, Tirupati 517507, India*

19 February 2024

ABSTRACT

Superthin galaxies are a class of bulgeless, low surface brightness galaxies with strikingly high values of planar-to-vertical axes ratio ($b/a > 10-20$), possibly indicating the presence of an ultra-cold stellar disc. Using the multi-component galactic disc model of gravitationally-coupled stars and gas in the force field of the dark matter halo as well as the stellar dynamical code AGAMA (Action-based Galaxy Modelling Architecture), we determine the vertical velocity dispersion of stars and gas as a function of galacto-centric radius for five superthin galaxies (UGC 7321, IC 5249, FGC 1540, IC2233 and UGC00711) using observed stellar and atomic hydrogen (HI) scale heights as constraints, using a Markov Chain Monte Carlo Method. We find that the central vertical velocity dispersion for the stellar disc in the optical band varies between $\sigma_{0s} \sim 10.2-18.4 \text{ kms}^{-1}$ and falls off with an exponential scale length of 2.6 to 3.2 R_d where R_d is the exponential stellar disc scale length. Interestingly, in the $3.6 \mu\text{m}$, the same, averaged over the two components of the stellar disc, varies between 5.9 to 11.8 kms^{-1} , both of which confirm the presence of “ultra-cold” stellar discs in superthin galaxies. Interestingly, the global median of the multi-component disc dynamical stability parameter Q_N of our sample superthins is found to be 5 ± 1.5 , which higher than the global median value of 2.2 ± 0.6 for a sample of spiral galaxies.

Key words: galaxies: disc, galaxies: ISM, galaxies: spiral, galaxies: structure, galaxies: kinematics & dynamics, Physical Data & Processes: instabilities

1 INTRODUCTION

Superthin galaxies are a class of edge-on disc galaxies exhibiting extra-ordinarily high values of planar-to-vertical axes ratio $b/a \sim 10-20$, with no discernible bulge component. They are generally characterized by low values of central B -band surface brightness $\mu_B \sim 23-26 \text{ magarcsec}^{-2}$, low star formation rates $\sim 0.01 - 0.05 M_{\odot}\text{yr}^{-1}$, gas richness as indicated by high values of the ratio of the total neutral hydrogen (HI) mass to the total B -band luminosity $M_{HI}/L_B \sim 1$ and dark matter dominance at all galacto-centric radii. Superthins are therefore classic examples of under-evolved systems and ideal test-beds of galaxy formation and evolution processes in the local universe (See [Matthews et al. \(1999b\)](#) for a review).

The term *superthin* was first introduced by [Goad & Roberts \(1981\)](#) who did a spectroscopic study of four edge-on galaxies: UGC 7321, UGC 7170, UGC 9242 and UGC 4278 (IC 2233). Superthin galaxies were also studied as part of Flat Galaxy catalog (FGC) which was an optical survey of flat and bulgeless galaxies in the local universe; 1150 out of

4000 FGC galaxies were found to have $b/a > 10$ ([Karachentsev et al. 1993](#)). Later superthin galaxies have also been studied as part of the optical study of flat galaxies ([Kautsch 2009](#)) and, recently, very thin galaxies in the SDSS ([Bizyaev et al. 2016](#)). In addition, being rich in neutral hydrogen gas (HI), superthin galaxies have also been studied as of large HI surveys of edge-on disc galaxies. See, for example, [Giovanelli et al. \(1997\)](#) and [Matthews & van Driel \(2000\)](#).

The origin of a superthin stellar disc in these low surface brightness galaxies is still not well understood. The vertical scale height of the stellar disc in a disc galaxy is determined by a balance between the gradient of the stellar velocity dispersion in the vertical direction and the net vertical gravitational potential. Using their multi-component galactic disc model of gravitationally-coupled stars and gas in the force-field of the dark matter halo as constrained by the observed HI rotation curve and HI scale height, [Banerjee et al. \(2010\)](#) found that the superthin galaxy UGC7321 has a dense and compact dark matter halo i.e., $\frac{R_c}{R_d} \leq 2$ where R_c is the core radius of the pseudo-isothermal dark matter halo and R_d the exponential stellar disc scale length (See, also, [O’Brien et al. \(2010\)](#)). As a direct follow-up of this work, [Banerjee & Jog \(2013\)](#) showed that the compact dark matter halo is responsible for the existence of superthin disc in UGC 7321. Using

* E-mail: kaditya@students.iisertirupati.ac.in

† E-mail : arunima@iisertirupati.ac.in

stellar photometry and HI 21cm radio-synthesis, mass models of a few superthin galaxies were constructed using the observed HI rotation curve only: IC5249, IC2233 (Banerjee & Bapat 2017) and FGC1540 (Kurapati et al. 2018). In all these cases, it was found that $\frac{R_c}{R_d} \leq 2$, possibly indicating superthin galaxies are characterized by dense and compact dark matter halos in general, which, in turn, may strongly regulate the structure and dynamics of the galactic disc. Zasov et al. (1991) showed that a massive dark matter halo was responsible for suppressing bending instabilities in superthin galaxies. Using the 2-component disc dynamical stability parameter Q_{RW} proposed by Romeo & Wiegert (2011), Garg & Banerjee (2018) showed that the dark matter halo is responsible for the dynamical stability against local, axis-symmetric perturbations in a general sample of low surface brightness galaxies. Alternatively, given the fact that the morphology of disc galaxies is primarily driven by the angular momentum of their discs, the large planar-to-vertical axes ratios of the stellar discs in superthin galaxies may possibly be the outcome of a relatively higher value of the specific angular momentum of their discs. Jadhav Y & Banerjee (2019) however found that within the 95.4% confidence interval, some of the superthins does obey the same angular momentum-mass relation as ordinary disc galaxies, thus ruling out the role of the specific angular momentum as the primary factor in regulating the vertical structure of the superthin discs.

Finally, the origin of the superthin stellar disc may be possibly linked with small values of the vertical stellar velocity dispersion, which is indicative of minimal disc heating in a direction perpendicular to the galactic plane. Recent advances in Integral Field Unit (IFU) astronomy surveys have successfully estimated well-resolved stellar velocity dispersion for face-on or nearly face-on galaxies (Cappellari & others. (2011), Law et al. (2015), Allen et al. (2015), Bershadsky et al. (2010), Sánchez et al. (2012)). However, due to the edge-on geometry of the superthin galaxies, the direct determination of the vertical velocity dispersion is not feasible. In this paper, we use the multi-component galactic disc model of gravitationally-coupled stars and gas in the force field of the dark matter halo to constrain the vertical stellar dispersion for five superthin galaxies: UGC 7321, IC 5249, FGC 1540, IC2233 and UGC711 in the optical as well as the 3.6 μm using observed scale height data as constraint and employing the Markov Chain Monte Carlo (MCMC) method (Narayan & Jog 2002b). The mass models for the above galaxies constructed using stellar photometry and HI radio-synthesis observations were already available in the literature. Further, we check the consistency of our results from the multi-component model by using the publicly available stellar dynamical code Action-based Galaxy Modelling Architecture (AGAMA) of Vasiliev (2018). We use the best-fit stellar dispersion from the multi-component model as an input to AGAMA and determine the stellar vertical scale heights. We then compare it with the observed stellar scale height used to constrain the self-consistent model to check for the robustness of our results. Finally, we check the dynamical stability of our model galactic discs by calculating the multi-component disc stability parameters as proposed by Romeo & Wiegert (2011) and Romeo & Falstad (2013).

The paper is organized as follows: In §2 we introduce the dynamical models of the galaxy and the dynamical stability

parameters of the multi-component galactic discs, in §3, we describe the basic structural properties of our sample superthin galaxies and in the §4 the observational constraints for our each sample galaxy. In §5, we present our results and the corresponding discussion, followed by conclusions in §6.

2 DYNAMICAL MODEL OF THE GALAXY

2.1 The multi-component model

We model the galaxy as a multi-component system of gravitationally-coupled stars and HI gas, in the external force field of a dark matter halo. We further assume that the stars and gas are in vertical hydrostatic equilibrium and that their velocity dispersions remain constant in the z -direction. Finally, for reasons of simplicity, we assume that the stars and gas are confined in axisymmetric discs, which are coplanar and concentric with each other. The joint Poisson distribution for the above system in terms of galactic cylindrical coordinates (R, ϕ, z) is ;

$$\frac{\partial^2 \Phi_{\text{total}}}{\partial z^2} + \frac{1}{R} \frac{\partial}{\partial R} \left(\frac{R \partial \Phi_{\text{total}}}{\partial R} \right) = 4\pi G \left(\sum_{i=1}^n \rho_i + \rho_{DM} \right) \quad (1)$$

where Φ_{total} is the total gravitational potential due to the disc components and the dark matter halo and ρ_i is the density of the i^{th} disc component where $i = 1$ to n , n denoting the number of disc components. ρ_{DM} the density of the dark matter halo. For a galaxy with a flat rotation curve, the radial term drops out and the Poisson's equation reduces to

$$\frac{\partial^2 \Phi_{\text{total}}}{\partial z^2} = 4\pi G \left(\sum_{i=1}^n \rho_i + \rho_{DM} \right) \quad (2)$$

The equation of vertical hydrostatic equilibrium for the j^{th} component of the disc ($j = \text{stars, gas}$) (Rohlf 1977) is

$$\frac{\langle (\sigma_z)_j^2 \rangle}{\rho_j} \frac{\partial \rho_j}{\partial z} + \frac{\partial \Phi_{\text{total}}}{\partial z} = 0 \quad (3)$$

Combining the joint Poisson's equation and the equation for vertical hydrostatic equilibrium we get:

$$\frac{\partial^2 \rho_j}{\partial z^2} = \sum_{i=1}^n -4\pi G \frac{\rho_j}{\langle (\sigma_z)_j^2 \rangle} (\rho_i + \rho_{DM}) + \left(\frac{\partial \rho_j}{\partial z} \right)^2 \frac{1}{\rho_j}; \quad (4)$$

where ρ_j , j stands for the density and $\langle (\sigma_z)_j^2 \rangle$ is the vertical velocity dispersion of the j^{th} component with $j = 1$ to n . The dark matter is modelled as a pseudo-isothermal profile given by

$$\rho_{DM} = \frac{\rho_0}{\left(1 + \frac{m^2}{R_c^2}\right)} \quad (5)$$

where

$$m^2 = R^2 + \frac{z^2}{q^2} \quad (6)$$

(de Zeeuw & Pfenniger 1988) where ρ_0 is the central core density, R_c the core radius and q the vertical-to-planar axes ratio of the spheroidal the halo. For a spherical halo $q = 1$, oblate $q < 1$, prolate $q > 1$. We assume a spherical halo in this work. In our work, ρ_{DM} is an input parameter, which was already determined in earlier mass modelling studies.

The radial profile of the vertical velocity dispersion of each of the stellar disc components is parametrized as :

$$\sigma_{z,s}(R) = \sigma_{0s} \exp(-R/\alpha_s R_d) \quad (7)$$

Here σ_{0s} is the central value of the vertical velocity dispersion of the stars and α_s the radial scale length of the exponential fall-off of the same in units of the exponential disc scale length R_d . Both σ_{0s} and α_s are free parameters. This is closely following the work of [van der Kruit & Searle \(1981\)](#), who modelled galactic discs of a sample of edge-on disc galaxies as self-gravitating with a vertical velocity dispersion remaining constant with z , and found $\alpha_s = 2$. However, low surface brightness galaxies like the superthins are gas-rich as well as dark matter dominated and hence cannot be modelled as self-gravitating discs. Hence, although we adopt the above parametric form for the radial profile of the vertical velocity dispersion of the stars for our sample superthins, we keep α_s as a free parameter in our model. Finally, the radial profile of the HI vertical velocity dispersion is parametrized as a polynomial as follows:

$$\sigma_{z,HI}(R) = \sigma_{0HI} + \alpha_{HI}R + \beta_{HI}R^2 \quad (8)$$

with σ_{0HI} , α_{HI} and β_{HI} as free parameters. This is similar to the parametrizations adopted in modelling the HI velocity dispersion in M31 ([Narayan et al. 2005](#)) and in the Milky Way ([Banerjee & Jog 2008](#)). In some cases, the above profile may give a bad fit to the observed data and therefore we had to use a different profile as given below in order to get a better fit with the observed data.

$$\sigma_{z,HI}(R) = \sigma_{0HI} e^{-R/\alpha_{HI}} \quad (9)$$

with σ_{0HI} and α_{HI} as free parameters Equation (4) thus represents n coupled, non-linear ordinary differential equations in the variables ρ_i where $i = 1$ to n . For a given set of values of the free parameters, the above equation determines ρ_i 's as a function of z and hence scaleheight for all i at any R . The parameter values and hence the velocity dispersion profiles are constrained by the observed scale height values. The above equation is solved iteratively using the Runge-Kutta method with boundary conditions at midplane $z = 0$ given by;

$$\frac{d\rho_i}{dz} \quad (10)$$

and

$$\rho_i = (\rho_0)_i \quad (11)$$

However, ρ_i at $z = 0$ is not known a priori. Instead the surface density $\Sigma_i(R)$ (See equations 24 to 26 in section 4), which is given by twice the area under curve of $\rho_i(z)$ versus z , is used as the second boundary condition, since $\Sigma_i(R)$ can be observationally determined. Hence the required value of $\rho_i(0)$ can be then fixed by trial and error method, which eventually determines the $\rho_i(z)$ distribution. The above method has been used to study vertical density distribution of stars and gas in a host of disc galaxies as in [Narayan & Jog \(2002a\)](#), [Narayan et al. \(2005\)](#), [Banerjee & Jog \(2007\)](#), [Banerjee & Jog \(2008\)](#), [Banerjee et al. \(2010\)](#), [Banerjee & Jog \(2011b\)](#), [Banerjee & Jog \(2011a\)](#), [Banerjee & Jog \(2013\)](#), [Sarkar & Jog \(2019\)](#).

Model Fitting using Markov Chain Monte Carlo Method:

Since the parameter space to be scanned to obtain the best-fitting model is higher (4 – 7) dimensional (§4), we use the Markov Chain Monte Carlo (MCMC) method for determining the best-fitting set of parameters of our model. We use the task modMCMC from the publicly available R package FME ([Soetaert et al. 2010](#)), which implements MCMC using adaptive Metropolis procedure ([Haario et al. 2006](#))

Mean vertical stellar velocity dispersion: As we will see in §4, a stellar disc may be represented as a superposition of two exponential discs in a given photometric band. We will represent the mean velocity dispersion of such a stellar disc by introducing the density averaged mean dispersion given by:

$$\sigma_{z,s(avg)}^2 = \frac{\rho_1 \sigma_{z1}^2 + \rho_2 \sigma_{z2}^2}{\rho_1 + \rho_2} \quad (12)$$

the subscripts 1 and 2 denoting disc 1 and disc 2 respectively.

2.2 AGAMA

We use the publicly available stellar dynamical code AGAMA by [Vasiliev \(2018\)](#)¹ for an alternative dynamical modelling our sample of galaxies. Here we model each stellar disc at a time, assuming that it responds to the composite gravitational potential of all the disc components and the dark matter halo. We assume a double exponential profile for the same i.e. with exponential density distribution in the radial as well as in the vertical direction. We assume the HI component as having an exponential radial surface density profile with a constant scale height. The dark matter halo is modelled to have a pseudo-isothermal density profile. We then bind together all the dynamical components to construct a composite potential. We then initialize a quasi-isothermal distribution function for the stellar disc with the composite potential and the requisite structural parameters of the stellar disc, including the stellar velocity dispersion as obtained from our multi-component galactic disc model. The distribution function and the composite potential are then combined with an action finder for constructing a galaxy model with a single stellar population responding to the net underlying gravitational potential of the galaxy. The quasi-isothermal distribution function (DF) is given by

$$f(J) = f_0(J_\phi) \frac{\kappa}{\sigma_{R,s}^2} e^{-\frac{\kappa J_R}{\sigma_{R,s}^2}} \frac{\nu}{\sigma_{z,s}^2} e^{-\frac{\nu J_z}{\sigma_{z,s}^2}} \quad (13)$$

where κ and ν are the radial and vertical epicyclic frequencies respectively. $\sigma_{R,s}$ and $\sigma_{z,s}$ are the stellar velocity dispersions in the R and z directions respectively. J_R , J_z and J_ϕ are the actions of the stellar discs in the R , z and ϕ directions respectively. Here $J_\phi^2 = R^3 \frac{\partial \Phi}{\partial R}$ and $J^2 = J_R^2 + J_\phi^2 + J_z^2$. Moments of the density function may be computed as follows: The stellar density is given by

$$\rho_s(x) = \int \int \int d^3v f(J[x, v]) \quad (14)$$

¹ <https://github.com/GalacticDynamics-Oxford/Agama>

The mean stellar velocity is given by

$$\bar{v} = \frac{1}{\rho_s} \int \int d^3v v f(J) \quad (15)$$

while the second moment of stellar velocity is given by

$$\overline{v_{ij}^2} = \frac{1}{\rho} \int \int d^3v v_i v_j f(J) \quad (16)$$

Hence the velocity dispersion tensor is defined as

$$\sigma_{s,ij}^2 = \overline{v_{ij}^2} - \bar{v}_i \bar{v}_j \quad (17)$$

Each stellar disc is modeled using a 'Disk' type potential. The density distribution due to the disk type potential is given by

$$\rho_s = \Sigma_{0s} \exp\left(-\left[\frac{R}{R_d}\right]^{\frac{1}{n}} - \frac{R_{cut}}{R}\right) \times \begin{cases} \delta(z) & \text{if } h_z = 0 \\ \frac{1}{2h_z} \exp\left(-\left|\frac{z}{h_z}\right|\right) & h_z > 0 \\ \frac{1}{4|h_z|} \text{sech}^2\left(\left|\frac{z}{2h_z}\right|\right) & h_z < 0 \end{cases} \quad (18)$$

where Σ_{0s} is the central surface brightness, R_d is the disc scale length, h_z is the disc scale height, R_{cut} is the disc inner cut-off and n the sersic index. The HI component is modeled with a 'Disk' type density profile, with sersic index $n = 0.5$ and using the average HI scaleheight. The dark matter density is modeled using 'Spheroid' type potential with $\alpha = 2$, $\gamma = 0$, and $\beta = 2$ where 'spheroid' type density is given by

$$\rho = \rho_0 \left(\frac{\tilde{r}}{a}\right)^{-\gamma} \left[1 + \left(\frac{\tilde{r}}{a}\right)^\alpha\right]^{\frac{\gamma-\beta}{\alpha}} \times \exp\left[-\left(\frac{\tilde{r}}{r_{cut}}\right)^\xi\right] \quad (19)$$

where ρ_0 is the central density and a the core radius. We add together the above densities to create a total density profile of the galaxy. Then we use the 'GalaxyModel' function to create a composite model of the galaxy using the total density profile and the quasi-isothermal distribution for the disc component. Using the tasks 'moments' and 'projectedMoments' we compute the radial and vertical stellar dispersion profiles and the scale height of the stellar disc. We note here we do not employ the iterative method for constructing self-consistent equilibrium configurations, but simply initialize a DF in the given composite potential of all the disc components and the dark halo.

Multi-component galactic disc model versus AGAMA model:

We note here, we are comparing two approaches for computing the stellar vertical dispersion: one is based on the Jeans' equations for hydrostatic equilibrium, generalized to include multiple components i.e, both stars and gas, and the other on computing the moments of a distribution function in the given potential. Both methods are based on the equilibrium assumption, but differ in details. The common limitation of the former method is the neglect of radial gradients i.e. the resulting ordinary differential equation is solved in z direction independently at each R , and the latter method is in principle more general and accurate, but as long as the potential is indeed computed self-consistently from the DF. In that case, the full set of Jeans equations (and not just the vertical one) should be satisfied automatically. However, the caveat is the density profile generated by the DF does not necessarily follow the exponential law, although it should be reasonably close if the parameters of the DF were chosen correctly, and if the system is not too hot. The other important parameters of the DF are the central value of radial velocity dispersion, and the scale length of its fall off

which cannot be obtained from the multi-component model directly, in a self-consistent manner. We note here we do not employ the iterative method for constructing self-consistent equilibrium configurations, but simply initialize a DF in the given composite potential of all the disc components and the dark halo. This approach will give reasonable results, provided the parameters of the DF are in agreement with the parameters of the stellar density profile (i.e., central surface density, scale radius, scale height are the same in the Disk density profile and in the QuasiIsothermal DF) which has been ensured in this work.

2.3 Disc dynamical stability

The disc stability against local axis-symmetric perturbations is determined by the a balance between the self-gravity on one hand and combined effect of velocity dispersion and the centrifugal force due to coriolis spin up of the perturbations on the other hand. The Q parameter (Toomre 1964) for a one component rotating fluid discs is

$$Q = \frac{\kappa \sigma_R}{\pi G \Sigma} \quad (20)$$

where κ is the epicyclic frequency given by $\kappa^2 = -4B\Omega$. B and Ω are the Oort constant and the angular frequency respectively, σ_R is the radial velocity dispersion and Σ the surface density at a given radius R . A value of $Q > 1$ implies a stable disc and $Q \leq 1$ is indicative of an unstable galactic disc which is characteristic of star-forming regions. Superthin galaxies are rich in gas, which may strongly regulate the disc dynamics closer to the midplane (Banerjee & Jog 2007). Hence, the galactic disc can no more be considered as a single component self-gravitating disc. We use multi component stability parameter Q_N derived by Romeo & Falstad (2013) for studying the stability of the galaxy disc in $3.6\mu m$ where the galaxies are composed of two stellar discs and a HI, discs. The effective stability parameter Q_N for a multi-component galaxy disc is defined as

$$\frac{1}{Q_N} = \sum_{i=1}^N \frac{W_i}{T_i Q_i} \quad (21)$$

The thickness of the galaxy disc increases the effective stability of the galaxy disc and is parameterized as

$$T \approx \begin{cases} 1 + 0.6\left(\frac{\sigma_z}{\sigma_R}\right)^2 & \text{if } 0 \leq \frac{\sigma_z}{\sigma_R} \leq 0.5 \\ 0.8 + 0.7\left(\frac{\sigma_z}{\sigma_R}\right) & \text{if } 0.5 \leq \frac{\sigma_z}{\sigma_R} \leq 1 \end{cases} \quad (22)$$

The weight factor for the Q_N is defined as

$$W_i = \frac{2\sigma_m \sigma_i}{\sigma_m^2 + \sigma_i^2} \quad (23)$$

Where i is the i^{th} component of the galaxy and m is the component with smallest TQ i.e $T_m Q_m = \min(T_i Q_i)$. We note that $Q_{RW} = 1$ or $Q_N = 1$ gives the critical stability level of a galactic disc in the presence of local, axi-symmetric perturbations only. However, real galactic discs are not subjected to local, axisymmetric perturbations alone. In fact, non-axisymmetric perturbations are primarily responsible for the formation of bars and spiral arms in galactic discs. Griv & Gedalin (2012a) showed that non-axisymmetric perturbations have a destabilizing effect and therefore may increase the critical stability threshold for local axisymmetric perturbations to $Q_{RW} \sim 1 - 2$ (Romeo & Fathi 2015). In addition

to this, there may be gas dissipation effects, which may raise the critical stability level further to $Q_{RW} \sim 2$ -3 (Elmegreen 2011a). Therefore, in this work, we consider a galactic disc to be dynamically stable if Q_{RW} or Q_N is between 2 and 3.

3 SAMPLE OF SUPERTHIN GALAXIES

In order to constrain the vertical velocity dispersion, we need a sample of galaxies with observed stellar and HI scaleheight. As input parameters to the two-component model and for calculating the potential for setting up an equilibrium distribution function in AGAMA, we need the stellar and HI densities and along with the dark matter density as a function of the galactocentric radius. Thus, we have chosen our sample of superthin galaxies based on the availability of the three dimensional stellar photometry in optical and 3.6 μm band along HI surface densities and mass models derived from high resolution HI 21 cm line observations.

3.1 UGC7321

UGC 7321 is a prototypical nearby superthin galaxy at a distance $D = 10$ Mpc (Matthews 2000), inclination $i = 88^\circ$ (Matthews et al. 1999a) and major-to-minor axes ratio $b/a = 10.3$. Its characterized by a steeply rising rotation curve with an asymptotic velocity $\sim 110 \text{ km s}^{-1}$ (Uson & Matthews 2003). The deprojected central surface brightness in B-band is $23.5 \text{ mag arcsec}^{-2}$ (Matthews et al. 1999a). The galaxy has large dynamical mass $M_{dyn}/M_{HI} = 31$ and $M_{dyn}/L_B = 29$ (Roberts & Haynes 1994) which underscores the importance of the dark matter in these galaxies. Constraining the dark matter halo of UGC7321 using observed HI rotation curve and HI vertical scaleheight data revealed a compact dark matter with $\rho_0 = 0.039 M_\odot \text{ pc}^{-3}$ and $R_c = 2.9 \text{ kpc}$ (Banerjee et al. 2010). See, also, Banerjee & Bapat (2017).

3.2 IC 5249

IC 5249 is an edge-on galaxy observed at an inclination $i = 89^\circ$ (Abe et al. 1999) with axial ratio $b/a = 10.2$. The galaxy has an asymptotic rotational velocity of about 112 km s^{-1} . The $M_{dyn}/M_{HI} = 9.5$ and $M_{dyn}/L_B = 9.5$ (Yock et al. (1999), van der Kruit et al. (2001)). Mass modelling of IC 5249 indicated the presence of a dark matter halo with $R_c = 2.9 \text{ kpc}$ and $\rho_0 = 0.026 M_\odot \text{ pc}^{-3}$ (Banerjee & Bapat 2017).

3.3 FGC 1540

FGC 1540 is a superthin galaxy at a distance of $D = 10$ Mpc. It is observed at an inclination of $i = 87^\circ$ and has an axial ratio $b/a = 7.5$. It is classified as a superthin in the Flat galaxy catalogue (Karachentsev et al. 1993). It has $M_{HI}/L_B = 4.1$ and is characterised by an asymptotic rotational velocity of about 90 km s^{-1} and the mass modelling indicates a central dark matter density $\rho_0 = 0.262 M_\odot \text{ pc}^{-3}$ and a core radius 0.69 kpc (Kurapati et al. 2018).

3.4 IC 2233

IC 2233 is a superthin galaxy with an axial ratio $b/a = 7$, observed at an inclination of 88.5° (Matthews & Uson 2007) at a distance of 10 Mpc. The galaxy has an asymptotic rotational velocity of about 85 km s^{-1} . $M_{HI}/L_b \sim 0.62$ and the $M_{dyn}/M_{HI} \sim 12$, the latter indicating that the galaxy is rich in HI. Mass models predicts a central dark matter density $\rho_0 = 0.055 M_\odot \text{ pc}^{-3}$ and a core radius 1.83 kpc (Banerjee & Bapat 2017).

3.5 UGC00711

UGC0711 is a superthin galaxy with a planar-to-vertical axial ratio $b/a = 15.5$ and observed at an inclination of 74.7° at a distance of $D = 23.4$ Mpc. The galaxy has an asymptotic rotational velocity of $\sim 100 \text{ km s}^{-1}$ (Mendelowitz et al. 2000). Mass modelling predicts a central dark matter density $\rho_0 = 0.033 M_\odot \text{ pc}^{-3}$ and a characteristic core radius 2.95 kpc (Banerjee & Bapat 2017).

4 OBSERVATIONAL CONSTRAINTS

We model the vertical stellar dispersion of the superthin galaxies in optical and in the 3.6 μm band using observed stellar and HI scaleheight as a constraint. The stellar disc appears superthin in optical, which, in turn, traces the young stellar population. The 3.6 μm band, on the other hand, traces a relatively older stellar population which also constitutes the major mass fraction of the stellar component. More importantly, is free from dust extinction. Except for FGC1540, all our sample superthins are characterized by a single exponential stellar disc in the optical. Similarly, in the 3.6 μm band, except for UGC711, our sample galaxies are found to consist of two exponential stellar discs. Therefore, for our sample stellar discs, the surface density is either a single exponential given by

$$\Sigma_s(R) = \Sigma_{s0} \exp(-R/R_d) \quad (24)$$

where Σ_{s0} is the central stellar surface density and R_d the exponential stellar disc scale length. or, a double exponential given by

$$\Sigma_s(R) = \Sigma_{01} \exp(-R/R_{d1}) + \Sigma_{02} \exp(-R/R_{d2}) \quad (25)$$

where Σ_{01} is the central stellar surface density and R_{d1} the exponential stellar disc scale length of stellar disc 1 and so on. However, we may note here a recent study of UGC7321 showed that a double disc is not required to explain the data and argued that physically the existence of a second, thick disk in superthin galaxies is debatable (Sarkar & Jog 2019). The structural parameters for the stellar disc, i.e., the central surface density, the disc scale length and the scale height for UGC 7321 in B-band were taken from Uson & Matthews (2003). For IC5249, structural parameters for the disc were not available in the literature. For FGC1540, the i -band parameters were taken from Kurapati et al. (2018). For IC2233, the same in r -band were obtained from Bizyaev et al. (2016). Finally, the data for UGC711 in B-band were taken from Mendelowitz et al. (2000). The structural parameters of the stellar discs of our sample galaxies in the optical band are summarized in Table 1. In 3.6 μm band, all our sample

Table 1. Input parameters for the model arising from the observational constraints

Parameters Galaxy	μ_{01}^1 $mag \ arcsec^{-2}$	Σ_{01}^2 $M_{\odot} \ pc^{-2}$	R_{d1}^3 kpc	h_{z1}^4 kpc	μ_{02}^5 $mag \ arcsec^{-2}$	Σ_{02}^6 $M_{\odot} \ pc^{-2}$	R_{d2}^7 kpc	h_{z2}^8 kpc	ρ_0^9 $M_{\odot} \ pc^{-3}$	R_c^{10} kpc
Structural properties in optical band										
UGC 7321	-	-	-	-	23.5	34.7	2.1	0.150	0.039	2.99
FGC 1540	21.67	33.14	1.29	0.675	20.60	88.79	1.29	0.185	0.308	0.64
IC 2233	22.90	17.85	2.47	0.332	-	-	-	-	0.0457	1.84
UGC 00711	-	15.0	1.6	0.317	-	-	-	-	0.05	2.9
Structural properties in 3.6 μm										
UGC 7321	21.73	7.165	2.39	0.436	19.9	37.26	1.0	0.134	0.140	1.27
IC 5249	21.7	5.44	5.24	0.724	20.53	15.97	1.23	0.253	0.026	2.99
FGC 1540	22.23	3.37	1.85	0.43	21.39	8.167	0.54	0.152	0.319	0.63
IC 2233	21.67	5.59	2.16	0.39	20.53	12.2	0.81	0.08	0.055	1.83
UGC 00711	-	14.6	2.14	0.44	-	-	-	-	0.033	2.95
Parameters of HI disc										
Parameters	Σ_{01}^{HI11} $M_{\odot} \ pc^{-2}$	$R_{0,1}^{12}$ kpc	a_1^{13} kpc	Σ_{02}^{HI14} $M_{\odot} \ pc^{-2}$	$R_{0,2}^{15}$ kpc	a_2^{16} kpc				
UGC 7321	4.912	2.85	3.85	2.50	1.51	0.485				
IC 5249	3.669	3.35	5.92	4.85	4.05	17.06				
FGC 1540	4.09	5.73	2.48	1.3	5.73	5.08				
IC 2233	2.236	1.79	2.52	2.454	1.69	6.14				
UGC 00711	30.83	3.73								

- (1): Central surface brightness of disc(1)
(2): Central stellar surface density disc(1)
(3): Exponential scale length for disc(1)
(4): Exponential scale height for disc(1)
(5): Central surface brightness of disc(2)
(6): Central stellar surface density disc(2)
(7): Exponential scale length for disc(2)
(8): Exponential scale height for disc(2)
(9): Core density of the pseudo-isothermal dark matter halo
(10): Core radius of the pseudo-isothermal dark matter halo
(11): The central surface density of disc 1 constituting the double gaussian HI profile
(12): Scalelength of gaussian disc(1)
(13): Offset in the centre of disc(1)
(14): The central surface density of disc 2 constituting the double gaussian HI profile
(15): Scalelength of gaussian disc(2)
(16): Offset in the centre of disc(2)

galaxies were found to have a thick and thin stellar disc, each with an exponential surface density and constant scale-height. The structural parameters for the same were taken from [Salo et al. \(2015\)](#) and are presented in Table 1. To sum up, among our sample galaxies, only UGC7321, UGC00711, and IC2233 are characterised by a single exponential disc in the optical band, but a pair of exponential discs in the 3.6 μ band. It is interesting to observe that the scale lengths of the optical discs of the above galaxies are closer to those of the thick disc component in the 3.6 μm band. However, their central surface densities and vertical scale heights in the optical band are closer to those of the thin disc component in the 3.6 μ band. This already indicates that there is perhaps no direct correspondence between the optical disc and any of the components of the 3.6 μm stellar disc for the above galaxies. FGC 1540 is characterised by a pair of exponential discs in both the optical and the 3.6 μm band. The radial scale lengths of the two discs in the optical have the same

value, and are close to the value of that of the thick disc in the 3.6 μm band. However, there is a significant mismatch between the surface density and the scale height values of the components in the optical and the 3.6 μm band. Finally, UGC711 is characterised by a single exponential disc both in the optical as well as in the 3.6 μm band, and the parameters seem to be fairly comparable to each other, possibly indicating that the disc is one and the same only in this case.

For UGC 7321, the HI surface density was taken from [Uson & Matthews \(2003\)](#), for IC 5249 from [van der Kruit et al. \(2001\)](#), for FGC 1540 from [Kurapati et al. \(2018\)](#), for IC2233 from [Matthews & Uson \(2007\)](#) and for UGC711 [Mendelowitz et al. \(2000\)](#). Earlier work indicated that the radial profiles of HI surface density could be well-fitted with double-gaussians profiles (See, for example, [Patra et al. \(2014\)](#)), possibly signifying the presence of two HI discs. Also, galaxies with the HI surface density peaking away from the centre are common, which indicates the presence of an

HI hole at the centre. Our sample HI surface density profiles could therefore be fitted well with off-centred double Gaussians given by

$$\Sigma_{HI}(R) = \Sigma_{01}^{HI} \exp\left[-\frac{(R-a_1)^2}{2R_{0,1}^2}\right] + \Sigma_{02}^{HI} \exp\left[-\frac{(R-a_2)^2}{2R_{0,2}^2}\right] \quad (26)$$

where Σ_{01}^{HI} is the central gas surface density, a_1 the centre and $R_{0,1}$ the scale length of gas disc 1 and so on. For the gas disc, we consider the atomic hydrogen (HI) surface density only as the presence of molecular gas in LSBs is known to be negligible (See, for example, Banerjee & Bapat (2017) for a discussion). The HI scaleheight for UGC 7321 and IC 5249 were obtained from O’Brien et al. (2010). For FGC 1540, we used approximately constant HI scaleheight of 0.400 kpc (Kurapati, private communication). HI scaleheight for the galaxy IC2232 and UGC711 was obtained by using the FWHM vs $\frac{2R}{D_{HI}}$ plot as given in O’Brien et al. (2010) as a scaling relation. We obtain FWHM = $\frac{2.4}{0.5D_{HI}}R + 0.244$, where D_{HI} is the HI diameter. We note here that due to the unavailability of observed HI scaleheight data, we have used rough estimates of the same in case of FGC1540, IC2233 and UGC711 in our calculations as discussed above. However, we stress that the HI scaleheight tightly constrains the value of HI velocity dispersion and not so much that of the stellar disc. So reasonable variation in the assumed value of the HI scaleheight will hardly change the best-fitting values of stellar vertical velocity dispersion as determined by our model. The parameters of the HI disc are summarized in Table 1.

For the stellar disc modelled using the optical band, the dark matter profile parameters i.e central core density ρ_0 and the core radius R_c for UGC 7321, was modelled by constructing mass models using the ‘rotmas’ and ‘rotmod’ tasks in gipsy (Van der Hulst et al. 1992). The same for FGC1540 were taken from Kurapati et al. (2018). For IC2233 and UGC711, the same were similarly modelled using gipsy. For the stellar disc modelled using the 3.6 μ m band, the dark matter profile parameters i.e central core density ρ_0 and the core radius R_c for UGC 7321, IC5249 and IC2233 were taken from Banerjee & Bapat (2017). The same for FGC1540 was obtained from Kurapati et al. (2018). For UGC711, the same was modelled using gipsy. In Table 1, we summarize the dark matter halo parameters of our sample superthins, with the stellar component modelled using the optical band. In Table 1, we summarize the same for the case in which the stellar component was modelled using the 3.6 μ m photometry. We note that the dark matter parameters obtained for the above two cases are quite different. As discussed, the 3.6 μ m band is a better representative of the stellar mass distribution. However, in order that our dynamical model is internally consistent, we use the dark matter parameters from the mass models constructed using a given photometry as input parameters in the dynamical equations determining the structure and kinematics of the stellar disc in a given photometric band.

5 RESULTS & DISCUSSION

5.1 Stellar vertical velocity dispersion

We present the results obtained from dynamical models of our sample of superthin galaxies as constrained by stellar photometry and HI 21cm radio-synthesis observations. In the figure 1, we present the vertical component of the stellar velocity dispersion in logarithmic scale $\log\sigma_z$ as a function of R/R_d obtained using the multi-component model of gravitationally-coupled stars and gas in the force field of the dark matter halo for our sample superthin galaxies. For each of our sample galaxies, we consider two different cases for the above dynamical model, depending on the choice of the photometric band to model the stellar component (i) Optical (ii) 3.6 μ . Except for FGC1540, our sample superthins is composed of a thin exponential stellar disc only in the optical-band. FGC1540, on the other hand, is composed of a thin and a thick stellar disc in the optical band. We note that in the optical band, the central value of the vertical component of the stellar velocity dispersion σ_{0s} (varies between 10.2 and 18.4 kms^{-1}).

In the 3.6 μ m band, the stellar component of all our sample galaxies, except for UGC711, is composed of a thin and a thick exponential stellar disc. UGC711 is composed of a thick disc only in the 3.6 μ m band. Interestingly, the central value of the vertical component of the stellar velocity dispersion σ_{0s} of the thin disc ranges between 3.9 to 9.3 kms^{-1} . The same for the thick disc varies between 15.9 to 24.7 kms^{-1} . The weighted average value for the thin and the thick stellar disc for the same lies between 5.9 to 11.6 kms^{-1} . The optical disc constitutes young stellar population whereas the 3.6 μ m band traces the older stellar population. We note that the thin disc component in 3.6 μ m band of UGC 7321, IC 5249, FGC 1540 and IC 2233 has a vertical stellar velocity dispersion, much lower than the corresponding value of the optical disc. We suspect that these galaxies might have undergone a recent star formation event, wherein the short lived young stars have passed on to the red giant phase, emitting in near-infrared. Thus, the thin disc in 3.6 μ m may represent this cold near-infrared component.

Previous studies on the vertical structure of disc galaxies mostly considered fixed values of $\alpha_s = 2$, in order to comply with a stellar scale height constant with radius (See for example Van der Kruit & Searle (1982), Van Der Kruit (1988), Van der Kruit & Freeman (2011), and also Sharma et al. (2014)). Following Narayan & Jog (2002a)), we consider α_s to be a free parameter. For the stellar discs in optical band, we find the value of α_s varies between 2.4 -3.7. For the 3.6 μ m band, the thick disc α_s varies between 2.1 -3.7. These values are in compliance with Narayan & Jog (2002a), who found α_s to be lying between 2 and 3. However, for the 3.6 μ m thin disc, α_s lies between 4.5 -12.1.

In comparison to our sample superthins, the value of the central vertical stellar velocity dispersion in the Milky Way (Lewis & Freeman 1989) and Andromeda (M31) (Tamm et al. 2007) are $\sim 53 \text{ kms}^{-1}$, assuming that the dispersion falls off with a scale length of $2R_d$, and that the ratio of vertical-to-radial stellar velocity dispersion equals 0.5 in solar neighbourhood (Binney & Merrifield 2008). Sharma et al. (2014) fitted kinematic models to the Radial Velocity Experiment (RAVE)(Steinmetz et al. 2006) and Geneva Copenhagen Survey (GCS) (Nordström et al. 2004) data

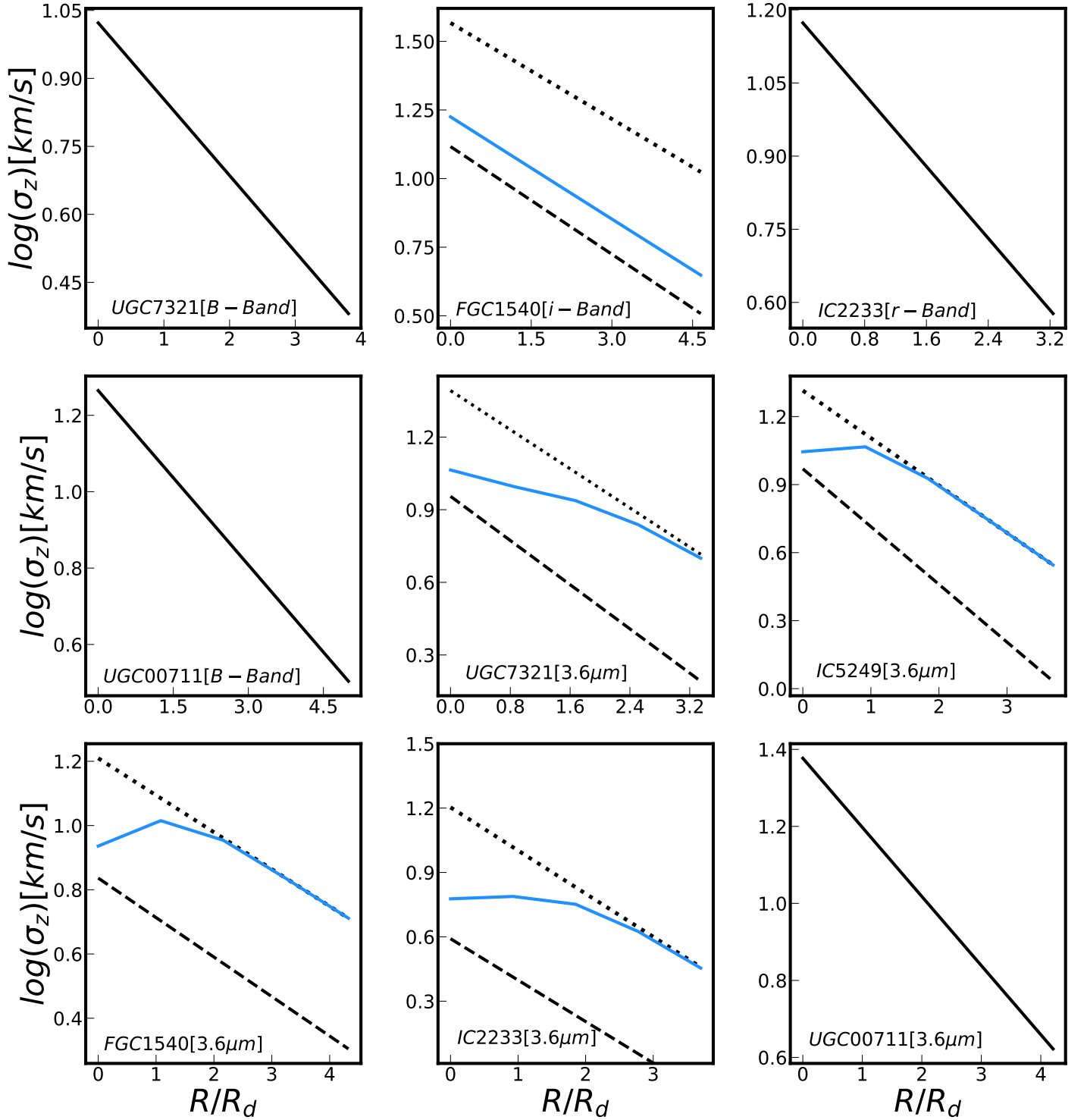


Figure 1. We plot our model-predicted stellar vertical velocity dispersion in logarithmic scale for our sample superthins as a function of galacto-centric radius R normalised by the exponential stellar disc scale length R_d . In case of 2-component stellar discs R_d corresponds to R_{d1} i.e., the scale length of the thick disc. In case of 1-component stellar disc, stellar vertical velocity dispersion is indicated by a single *solid* line. In case of 2-component discs, the *dashed* line corresponds to the thin disc, the *dotted* line to the thick disc and the *solid* line the density-averaged value of the same.

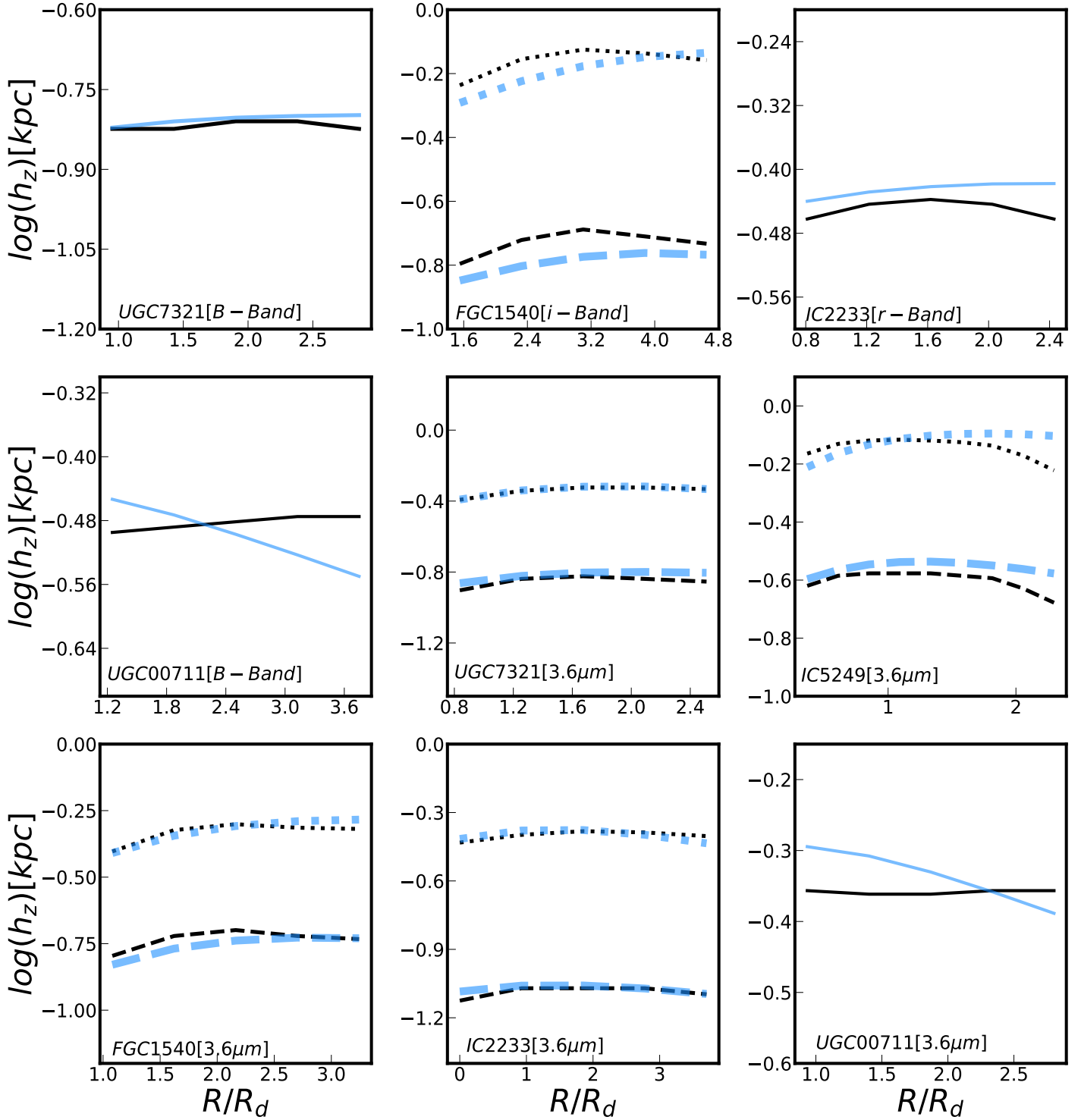


Figure 2. We plot our model-predicted stellar scaleheight in logarithmic scale for our sample superthins as a function of galacto-centric radius R normalised by the exponential stellar disc scale length R_d . In case of 2-component stellar discs R_d corresponds to R_{d1} i.e., the scale length of the thick disc. In case of 1-component stellar disc, stellar vertical scale height is indicated by a single *solid* line. In case of 2-component discs, the *dashed* line corresponds to the thin disc whereas the *dotted* line to the thick disc. The *black* lines correspond to the multi-component model whereas the *blue* lines to AGAMA.

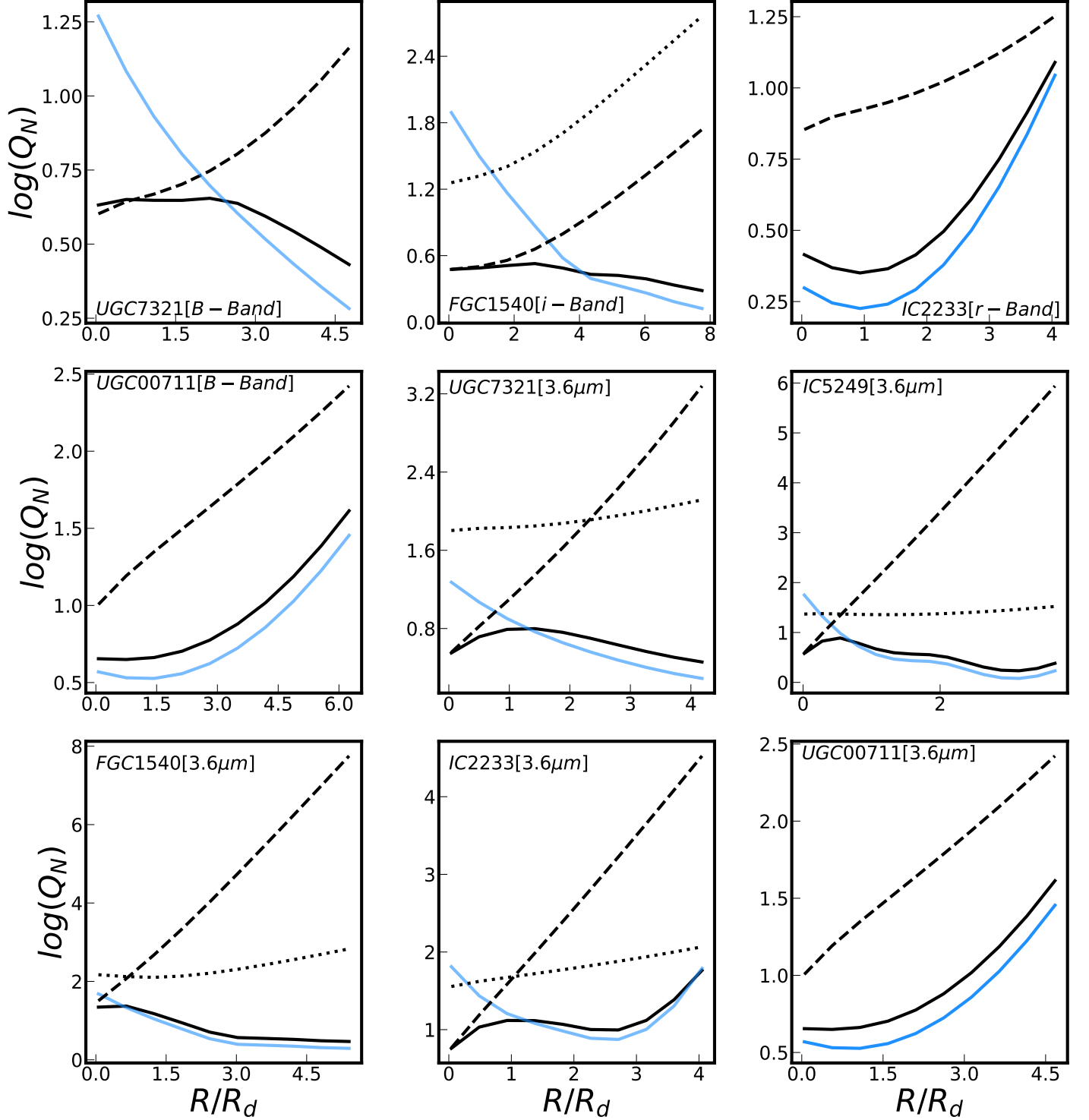


Figure 3. We plot our stability parameter Q_N in logarithmic scale for our sample superthins as a function of galacto-centric radius R normalised by the exponential stellar disc scale length R_d . In case of 2-component stellar discs R_d corresponds to R_{d1} i.e., the scale length of the thick disc. In case of 1-component stellar disc, the *dashed* line corresponds to the Toomre Q of the stellar disc. In case of a 2-component stellar disc, the *dashed* line corresponds to the Toomre Q of the thin disc whereas the *dotted* line to the Toomre Q of the thick disc. In both cases, the *blue* line corresponds to the Toomre Q of the gas disc whereas the *solid* line the multi-component disc stability parameter Q_N .

Table 2. Best-fitting parameters of the multi-component models of our sample superthin galaxies.

Parameters Galaxy	σ_{sI}^1 kms ⁻¹	α_{sI}^2	σ_{s0II}^3 kms ⁻¹	α_{sII}^4	σ_{avg}^5 kms ⁻¹
Vertical stellar dispersion: Stellar disc modelled using optical photometry .					
UGC 7321	-	-	10.23 ± 0.64	2.58 ± 0.613	
FGC 1540	36.91 ± 1.14	3.72 ± 0.4	13.08 ± 1.17	3.32 ± 0.42	16.78
IC 2233	14.9 ± 0.57	2.36 ± 0.36			
UGC 00711	18.4 ± 0.87	3.21 ± 0.40			
Vertical stellar dispersion: Stellar disc modelled 3.6 μm photometry.					
UGC 7321	24.66 ± 0.88	2.15 ± 0.6	9.02 ± 0.8	4.55 ± 0.68	11.58
IC 5249	20.64 ± 0.63	2.155 ± 0.217	9.32 ± 0.39	7.54 ± 0.23	11.08
FGC 1540	16.20 ± 0.87	3.77 ± 0.42	6.86 ± 0.57	12.1 ± 0.59	8.63
IC 2233	15.97 ± 0.54	2.16 ± 0.42	3.9 ± 0.23	6.0 ± 0.2	5.92
UGC 00711	23.82 ± 1.45	2.42 ± 0.28			
Vertical HI dispersion: Stellar disc modelled using optical photometry					
Parameters	σ_{0HI}^6 kms ⁻¹	α_{HI}^7	β_{HI}^8		
UGC 7321	11.06 ± 0.88	0.18 ± 0.07	-0.047 ± 0.02		
FGC 1540	29.01 ± 1.16	4.27 ± 0.425			
IC 2233	12.52 ± 0.515	1.03 ± 0.14	-0.141 ± 0.031		
UGC 00711	23.10 ± 1.11	1.03 ± 0.145	-0.156 ± 0.05		
Vertical HI dispersion: Stellar disc modelled 3.6 μm photometry.					
UGC 7321	11.19 ± 0.84	-0.29 ± 0.14			
IC 5249	12.4 ± 0.53	-0.99 ± 0.11	0.04 ± 0.0011		
FGC 1540	17.75 ± 0.81	6.85 ± 0.56			
IC 2233	12.0 ± 0.56	0.53 ± 0.23	-0.055 ± 0.026		
UGC 00711	22.03 ± 1.07	0.92 ± 0.16	-0.1 ± 0.054		

- (1): Central vertical stellar velocity dispersion in thick disc
(2): Scale length of radial fall off of the thick disc stellar dispersion in units of R_{d1}
(3): Central vertical stellar velocity dispersion in the thin disc
(4): Scale length of radial fall off of the thin disc stellar dispersion in units of R_{d2}
(5): Average stellar dispersion
(6): Central vertical HI dispersion
(7): steepness parameter-1 of HI dispersion profile
(8): steepness parameter-2 of HI dispersion profile

and found that the vertical velocity dispersion of the thin and thick disc of Milky Way stars are respectively given by $\sigma_{0sII} = 25.73^{+0.21}_{-0.21}$ km/s and $\sigma_{0sI} = 34.3^{+0.51}_{-0.57}$ km/s, the exponential scale lengths being $1/(\alpha_{s2}R_{d2}) = 0.073^{+0.0037}_{-0.003}$ kpc⁻¹ and $1/(\alpha_{sI}R_{d1}) = 0.1328^{+0.005}_{-0.0051}$ kpc⁻¹ respectively. In fact, the central vertical dispersion values of the older stellar population in two face-on spirals, NGC 628 and NGC 1566, are 60 km s⁻¹ and 80 km s⁻¹ respectively [Van der Kruit & Freeman \(1984\)](#), which are much higher than the range of 15 - 24 km s⁻¹ observed in the 3.6 μ m thick disc of our sample superthins. Compared to our sample of superthin galaxies the sample of 30 low inclination galaxies studied as part of the DiskMass survey have a central vertical dispersion in range 25.9 km s⁻¹ to 108.5 km s⁻¹ ([Martinsson et al. 2013](#)).

The multi-component model can simultaneously constrain the HI velocity dispersion of the galaxies as well. However, we had HI scale height measurements only for two of our sample galaxies: UGC 7321 and IC 5249. For the rest of the sample superthins, we estimated the HI scale height

using a scaling relation between the FWHM and HI diameter (see §4). Except for FGC1540, the HI velocity dispersion values obtained from the two different models of the stellar disc are comparable within error bars. We find that the HI dispersion for UGC 7321 and IC 5249 are 11.2 km/s and 12.4 km/s respectively, which roughly complies with the observed mean dispersion values 11.7 ± 2.3 km/s of nearby galaxies from the high-resolution THINGS HI surveys ([Mogotsi et al. 2016](#)). The central HI velocity dispersion of our superthin galaxy sample lies in range of 11 - 29 km s⁻¹. This roughly matches the findings of an earlier study of a sample of spiral galaxies in which the HI velocity dispersion was found to vary between 9 - 22 km s⁻¹ with a mean value of 11.7 km s⁻¹ [Mogotsi et al. \(2016\)](#). A similar value of HI velocity dispersion were observed by [Tamburro et al. \(2009\)](#) ~ 10 ± 2 km/s. We note that low values of HI dispersion are consistent with the cold neutral medium (CNM), having velocity dispersion in range 3.4 - 14.3 km s⁻¹ ([Ianjamasimanana et al. 2012](#)). Similarly, HI dispersion values on the higher side might possibly reflect presence of warm neutral medium (WNM) charac-

terised by values 10.4 - 43.2 kms⁻¹ (Ianjamasimanana et al 2012). Our calculations also indicate that the vertical velocity dispersion of the stellar disc is lower than that of the HI at some radii in some cases. It is, in general, not possible for the stars to have lower dispersion than the gas clouds in which they are formed as stars are collision less and therefore cannot dissipate energy through collisions. This possibly indicates that the thin disc stars were borne of very cold low dispersion molecular clouds, which could not be detected due to the very low metallicity of superthin galaxies. In the self-consistent model of gravitationally-coupled stars and gas, the vertical velocity dispersion of any component is tightly constrained by its own observed scale height value. Our model results have been summarised in Table 2.

5.2 Model stellar scaleheight : Multi-component model versus AGAMA

In the figure 2, we check the consistency of the multi-component model with the publicly-available stellar dynamical code AGAMA. Using the best-fitting value of the vertical stellar dispersion as obtained from the multi-component model as an input parameter in AGAMA, we find that the scale height predicted by AGAMA complies with that from the multi-component model. As discussed earlier, in contrast to the multi-component model, AGAMA determines the stellar radial velocity dispersion in addition to the vertical velocity dispersion, and thereby the ratio of the same as a function of galacto-centric radius. In the model constructed using optical band photometry for the stellar component, we find that the ratio of the vertical-to-planar velocity dispersion remains roughly constant at 0.5 within 3 R_d . On the other hand, in the model constructed using 3.6 micron photometry, our model indicates the following: For the thin disc, the ratio remains constant at 0.5 in UGC7321, IC5249 and UGC711; for FGC 1540, it varies between 0.5 and 0.3 whereas for IC2233 it remains constant at 0.3. For the thick disc, it remains constant at 0.5 in IC5249 and UGC711, at 0.3 in FGC1540 and varies between 0.4 and 0.3 in UGC7321 and IC2233. This is in line with the findings of Gerssen & Shapiro Griffin (2012), who showed that vertical-to-planar stellar velocity dispersion ratio decreases sharply from early-to-late-type galaxies. For an Sbc galaxy like the Milky Way, this value is ~ 0.5 . But for later-type galaxies like the superthins, it can be significantly closer to 0.3. Finally, we use the values of the radial stellar dispersion from AGAMA for testing the dynamical stability of our sample superthin galaxies.

5.3 Disc dynamical stability

In the figure 3, we plot the multi-component stability parameters Q_N derived of Romeo & Falstad (2013) as a function of R/R_d . We further superpose the Toomre parameter for each component of the disc on the same plot. We note that except for the innermost galactocentric radii, Q_N closely follows the Toomre parameter of the gas disc Q_g for all our sample galaxies in general.

In Figure 4, we present a composite plot of $\text{Log}Q_N$ versus R/R_d for our sample superthins. The Upper and the Lower Panels correspond to the cases in which the stellar

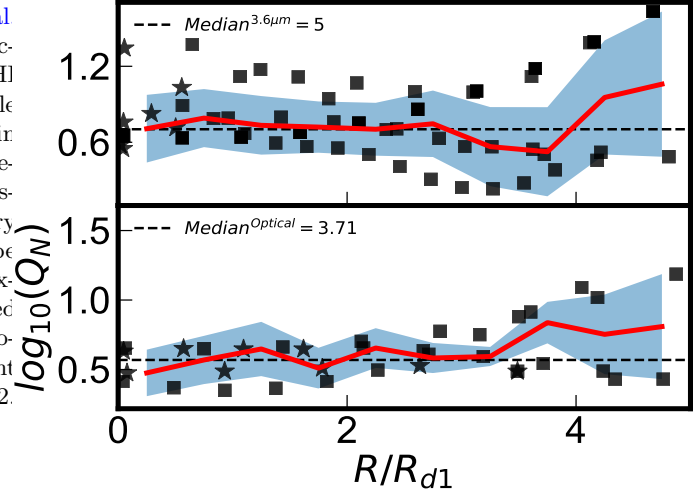


Figure 4. The figure presents the multi-component disc stability parameter Q_N of the our sample superthins as a function of galacto-centric radius R normalised by the exponential stellar disc scale length R_d . In case of 2-component stellar discs R_d corresponds to R_{d1} i.e., the scale length of the thick disc. Upper panel represents the case in which the stellar disc is modelled using 3.6 μ band whereas the lower panel the case corresponding to the optical band. `iStars` indicate the Q_N values driven by stellar disc and the `iSquares` those driven by the gas disc. The solid red line indicates the local median of the sample and the blue shaded region 1-sigma scatter about the median. The global median is indicated by the black dashed line.

disc is modelled using 3.6 μ m and optical photometry respectively. The local (solid line) and the global median (dotted) values of the sample are also indicated on the same plot. The blue shaded region represents the one sigma scatter of data points in each radial bin. The global median values for our superthin galaxies 5.0 ± 1.5 in the 3.6 μ m and 3.7 ± 1.5 in the optical band, these values are higher than the median Q_N of 2.2 ± 0.6 found for a sample of nearby star-forming galaxies by Romeo & Mogotsi (2017), who also modelled their stellar discs using 3.6 μ photometry from the SINGS survey (Kennicutt Jr et al. 2003). This possibly indicates that the superthins are dynamically stabler than ordinary disc galaxies in general. We further note that the global median values for our superthin galaxies is higher than the $Q_{critical} = 2$ (Griv & Gedalin 2012b), also higher than $Q_{critical} = 2-3$ derived by Elmegreen (2011b) taking into effect the destabilizing effect of gas dissipation. Our calculations show that in the optical band, the minimum Q_N values of our sample superthins range between 1.9 and 4.5 with a median of 2.5. In the 3.6 μ m band, the same varies between 1.7 and 5.7 with a median of 2.9. This complies with the median value 2.9 - 3.1 of the minimum Q_N for a sample of low surface brightness galaxies as found in earlier studies (Garg & Banerjee 2017).

5.4 How cold are superthin galaxies ?

So far we have only compared the absolute values of the vertical velocity dispersion of superthin galaxies as predicted by our theoretical model with those of ordinary galaxies. We found that the superthin galaxies are cold systems as compared to the massive spiral galaxies like Milkyway in terms of absolute vertical velocity dispersion. In Figure 5, we plot

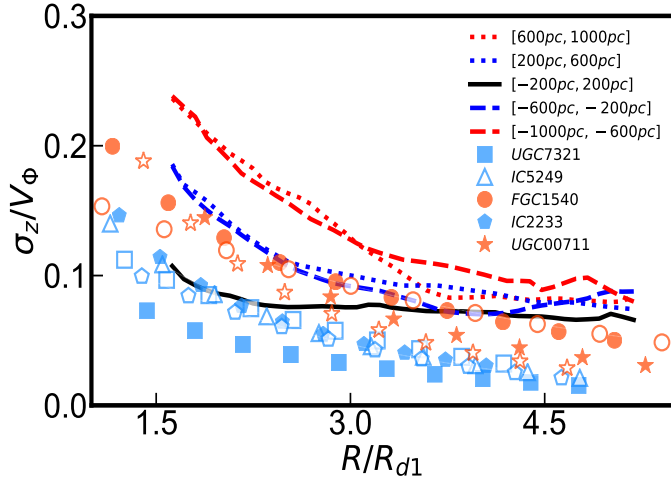


Figure 5. We plot the ratio of the vertical stellar velocity dispersion to the asymptotic rotational velocity σ_z/V_ϕ versus the galactocentric radius R normalised by R_d , the exponential stellar disc scale length for all our sample superthins. In case of 2-component stellar discs, σ_z corresponds to the density-averaged vertical velocity dispersion of the thin and the thick discs, and R_d corresponds to the thick disc scale length. The filled markers represent the optical band stellar disc models while the unfilled markers for the same marker-style the $3.6\mu\text{m}$ models. The solid and dotted lines of different colours denote the σ_z/V_ϕ versus R/R_d for the Milky Way stars corresponding to different vertical slices.

the vertical velocity dispersion of the thin stellar disc, both in the optical and in the $3.6\mu\text{m}$ band, normalized by their rotational velocity as a function of $R = Rd_1$. We compare the same with the corresponding with the corresponding profile of the Milky Way stars lying within different vertical heights from the galactic mid-plane as taken from [Katz et al. \(2018\)](#). Except at the inner radii of UGC00711 and FGC1540, the value of σ_z/V_ϕ for all the superthin galaxies is lower than than the corresponding value for the Milky Way stars in -200 pc to 200pc vertical slice, indicating the superthin galaxies are indeed ultra-cold systems.

Possible origin of the cold stellar discs in superthins

Bars, spiral arms, giant molecular clouds (GMCs) and satellite galaxies play an important role in heating the galactic disc. Spiral arms, on the other hand, heats the disc in the radial direction ([Aumer et al. 2016](#)). GMCs heat the disc in both vertical and radial direction ([Jenkins & Binney 1990](#)). [Saha \(2014\)](#) showed that galaxies hosting strong bars heat the disc very efficiently, leading to the formation of thick discs. Using N-body simulations, [Grand et al. \(2016\)](#) have shown that the time evolution of the bar strength correlates with the evolution of the global vertical energy of the stellar particles. In contrast, superthin galaxies possibly have weak bars which disfavour disc heating in the vertical direction and may thus preserve the superthin vertical structure. [Aumer et al. \(2016\)](#) finds that massive satellite galaxies and subhaloes also significantly heat the galactic disc in the vertical direction.

6 CONCLUSIONS

Superthin galaxies are a class of low surface brightness, bulgeless, disc galaxies, exhibiting sharp, needle-like images in the optical, implying strikingly high values of planar-to-vertical axes ratios of the stellar disc, which possibly indicates the presence of an ultra-cold stellar disc, the dynamical stability of which continues to be a mystery. We construct dynamical models of a sample of superthin galaxies using stellar photometry and HI 21cm radio-synthesis observations as constraints and employing a Markov Chain Monte Carlo method, also checking the consistency of our model results using AGAMA i.e. Action-based Galaxy Modelling Architecture ([Vasiliev 2018](#)).

- We find that the central vertical velocity dispersion for the stellar disc in the optical band varies between $\sigma_{0s} \sim 10.2 - 18.4 \text{ kms}^{-1}$ and falls off with an exponential scale length of 2.6 to 3.2 R_d where R_d is the exponential stellar disc scale length. Interestingly, in the $3.6\mu\text{m}$, the same, averaged over the two components of the stellar disc, varies between 5.9 to 11.8 kms^{-1} , which is mainly representative of the denser, thinner and smaller of the two-disc components. However, the dispersion of the more massive disc component varies between 15.9–24.7 with a scale length of $\sim 2.2 R_d$. Our results are indicative of the presence of ultra-cold stellar discs in superthin galaxies.

- We have constructed the stellar velocity ellipsoid (σ_z/σ_R) by setting up an equilibrium distribution function for our sample superthins using AGAMA. We find that the value of σ_z/σ_R lies in between 0.48 - 0.59 for optical models. σ_z/σ_R for thick disc in $3.6\mu\text{m}$ models varies between 0.4 - 0.55, the same for the thin disc lies between 0.28 - 0.51.

- Further, we find that the disc dynamical stability of super thin galaxies as indicated by Q_N is mainly driven by the gas component. Finally, in the $3.6\mu\text{m}$ band, the global median of the multi-component disc dynamical stability parameter Q_N of our sample superthins is found to be 5 ± 1.5 , which higher than the global median value of 2.2 ± 0.6 ([Romeo & Mogotsi 2017](#)) for a sample of spiral galaxies.

7 DATA AVAILABILITY

The data underlying this article are available in the article itself.

8 ACKNOWLEDGEMENT

AB would like to thank Prof. Francoise Combes for useful discussion, and Prof. Chanda Jog and Dr. Eugene Vasilev for useful comments and suggestions. AB would also acknowledge the research grant from DST-INSPIRE Faculty Fellowship (DST/INSPIRE/04/2014/015709) for partially supporting this work.

Softwares/Packages

We have used publically available R and python packages in this work. We have used FME ([Soetaert et al. 2010](#)) for

MCMC modelling, for analysis of results we relied on packages `ggmcmc` (Fernández-i Marín 2016), `BayesianTools` (Hartig et al. 2017), and for purpose of plotting we have used `ggplot2` (Wickham 2011), `Matplotlib` (Hunter 2007), `tonic` (Vaughan et al. 2016).

REFERENCES

- Abe F., et al., 1999, *The Astronomical Journal*, 118, 261
- Allen J., et al., 2015, *Monthly Notices of the Royal Astronomical Society*, 446, 1567
- Aumer M., Binney J., Schönrich R., 2016, *Monthly Notices of the Royal Astronomical Society*, 462, 1697
- Banerjee A., Bapat D., 2017, *Monthly Notices of the Royal Astronomical Society*, 466, 3753
- Banerjee A., Jog C. J., 2007, *The Astrophysical Journal*, 662, 335
- Banerjee A., Jog C. J., 2008, *The Astrophysical Journal*, 685, 254
- Banerjee A., Jog C. J., 2011a, *Monthly Notices of the Royal Astronomical Society*, 415, 687
- Banerjee A., Jog C. J., 2011b, *The Astrophysical Journal Letters*, 732, L8
- Banerjee A., Jog C. J., 2013, *Monthly Notices of the Royal Astronomical Society*, 431, 582
- Banerjee A., Matthews L. D., Jog C. J., 2010, *New Astronomy*, 15, 89
- Bershady M. A., Verheijen M. A. W., Swaters R. A., Andersen D. R., Westfall K. B., Martinsson T., 2010, *The Astrophysical Journal*, 716, 198–233
- Binney J., Merrifield M., 2008, *Galactic Astronomy*,
- Bizyaev D., Kautsch S., Sotnikova N. Y., Reshetnikov V. P., Mosenkov A. V., 2016, *Monthly Notices of the Royal Astronomical Society*, 465, 3784
- Cappellari M., others. 2011, *Monthly Notices of the Royal Astronomical Society*, 413, 813
- Elmegreen B. G., 2011a, *The Astrophysical Journal*, 737, 10
- Elmegreen B. G., 2011b, *The Astrophysical Journal*, 737, 10
- Fernández-i Marín X., 2016, *Journal of Statistical Software*, 70, 1
- Garg P., Banerjee A., 2017, *Monthly Notices of the Royal Astronomical Society*, 472, 166
- Garg P., Banerjee A., 2018, *Monthly Notices of the Royal Astronomical Society*, 472, 166
- Gerssen J., Shapiro Griffin K., 2012, *Monthly Notices of the Royal Astronomical Society*, 423, 2726
- Giovanelli R., Avera E., Karachentsev I., 1997, *arXiv preprint astro-ph/9704189*
- Goad J., Roberts M., 1981, *The Astrophysical Journal*, 250, 79
- Grand R. J., Springel V., Gómez F. A., Marinacci F., Pakmor R., Campbell D. J., Jenkins A., 2016, *Monthly Notices of the Royal Astronomical Society*, 459, 199
- Griv E., Gedalin M., 2012a, *Monthly Notices of the Royal Astronomical Society*, 422, 600
- Griv E., Gedalin M., 2012b, *Monthly Notices of the Royal Astronomical Society*, 422, 600
- Haario H., Laine M., Mira A., Saksman E., 2006, *Statistics and computing*, 16, 339
- Hartig F., Minunno F., Paul S., Cameron D., Ott T., 2017, *R package version. R package version 0.1, 3*
- Hunter J. D., 2007, *Computing in science & engineering*, 9, 90
- Ianjamasimanana R., De Blok W., Walter F., Heald G. H., 2012, *The Astronomical Journal*, 144, 96
- Jadhav Y V., Banerjee A., 2019, *Monthly Notices of the Royal Astronomical Society*, 488, 547
- Jenkins A., Binney J., 1990, *Monthly Notices of the Royal Astronomical Society*, 245, 305
- Karachentsev I., Karachentseva V., Parnovsky S., 1993, *Astronomische Nachrichten*, 314, 97
- Katz D., et al., 2018, *Astronomy & astrophysics*, 616, A11
- Kautsch S. J., 2009, *Publications of the Astronomical Society of the Pacific*, 121, 1297
- Kennicutt Jr R. C., et al., 2003, *Publications of the Astronomical Society of the Pacific*, 115, 928
- Kurapati S., Banerjee A., Chengalur J. N., Makarov D., Borisov S., Afanasiev A., Antipova A., 2018, *Monthly Notices of the Royal Astronomical Society*, 479, 5686
- Law D. R., et al., 2015, *The Astronomical Journal*, 150, 19
- Lewis J. R., Freeman K., 1989, in , *The World of Galaxies*. Springer, pp 202–205
- Martinsson T. P., Verheijen M. A., Westfall K. B., Bershady M. A., Schechtman-Rook A., Andersen D. R., Swaters R. A., 2013, *Astronomy & Astrophysics*, 557, A130
- Matthews L., 2000, *The Astronomical Journal*, 120, 1764
- Matthews L. D., Usón J. M., 2007, *The Astronomical Journal*, 135, 291
- Matthews L., van Driel W., 2000, *Astronomy and Astrophysics Supplement Series*, 143, 421
- Matthews L., Gallagher III J., Van Driel W., 1999a, *The Astronomical Journal*, 118, 2751
- Matthews L. D., van Driel W., Gallagher J. S., 1999b, *eprint arXiv astro-ph, 9911022v1*
- Mendelowitz C., Matthews L., Hibbard J., Wilcots E., 2000, in *Bulletin of the American Astronomical Society*. p. 1459
- Mogotsi K., de Blok W., Caldú-Primo A., Walter F., Ianjamasimanana R., Leroy A., 2016, *The Astronomical Journal*, 151, 15
- Narayan C. A., Jog C. J., 2002a, *Astronomy & Astrophysics*, 390, L35
- Narayan C. A., Jog C. J., 2002b, *Astronomy & Astrophysics*, 394, 89
- Narayan C. A., Saha K., Jog C. J., 2005, *Astronomy and Astrophysics*, 440, 523
- Nordström B., et al., 2004, *Astronomy & Astrophysics*, 418, 989
- O’Brien J. C., Freeman K., van der Kruit P., 2010, *Astronomy & Astrophysics*, 515, A62
- Patra N. N., Banerjee A., Chengalur J. N., Begum A., 2014, *Monthly Notices of the Royal Astronomical Society*, 445, 1424
- Roberts M. S., Haynes M. P., 1994, *Annual Review of Astronomy and Astrophysics*, 32, 115
- Rohlf K., 1977
- Romeo A. B., Falstad N., 2013, *Monthly Notices of the Royal Astronomical Society*, 433, 1389
- Romeo A. B., Fathi K., 2015, *Monthly Notices of the Royal Astronomical Society*, 451, 3107
- Romeo A. B., Mogotsi K. M., 2017, *Monthly Notices of the Royal Astronomical Society*, 469, 286
- Romeo A. B., Wiegert J., 2011, *Monthly Notices of the Royal Astronomical Society*, 416, 1191
- Saha K., 2014, *arXiv preprint arXiv:1403.1711*
- Salo H. L. E., et al., 2015, *The Astrophysical Journal Supplement Series*, 219, 4
- Sánchez S., et al., 2012, *Astronomy & Astrophysics*, 538, A8
- Sarkar S., Jog C. J., 2019, *arXiv preprint arXiv:1905.02735*
- Sharma S., et al., 2014, *The Astrophysical Journal*, 793, 51
- Soetaert K., Petzoldt T., et al., 2010, *Journal of Statistical Software*, 33, 1
- Steinmetz M., et al., 2006, *The Astronomical Journal*, 132, 1645
- Tamburro D., Rix H.-W., Leroy A., Mac Low M.-M., Walter F., Kennicutt R., Brinks E., De Blok W., 2009, *The Astronomical Journal*, 137, 4424
- Tamm A., Tempel E., Tenjes P., 2007, *arXiv preprint arXiv:0707.4375*

- Toomre A., 1964, *The Astrophysical Journal*, 139, 1217
- Uson J. M., Matthews L., 2003, *The Astronomical Journal*, 125, 2455
- Van Der Kruit P., 1988, *Astronomy and Astrophysics*, 192, 117
- Van der Hulst J., Terlouw J., Begeman K., Zwitter W., Roelfsema P., 1992, in *Astronomical Data Analysis Software and Systems I*. p. 131
- Van der Kruit P., Freeman K., 1984, *The Astrophysical Journal*, 278, 81
- Van der Kruit P., Freeman K., 2011, *Annual Review of Astronomy and Astrophysics*, 49, 301
- Van der Kruit P., Searle L., 1982, *Astronomy and Astrophysics*, 110, 61
- Vasiliev E., 2018, *Monthly Notices of the Royal Astronomical Society*, 482, 1525
- Vaughan S., Uttley P., Markowitz A., Huppenkothen D., Middleton M., Alston W., Scargle J., Farr W., 2016, *Monthly Notices of the Royal Astronomical Society*, 461, 3145
- Wickham H., 2011, *Wiley Interdisciplinary Reviews: Computational Statistics*, 3, 180
- Yock P., Pennycook G., Rattenbury N., Koribalski B., Muraki Y., Yanagisawa T., Jugaku J., Dodd R., 1999, in *The Third Stromlo Symposium: The Galactic Halo*. p. 187
- Zasov A., Makarov D., Mikhailova E., 1991, *Soviet Astronomy Letters*, 17, 374
- de Zeeuw T., Pfenniger D., 1988, *Monthly Notices of the Royal Astronomical Society*, 235, 949
- van der Kruit P. C., Searle L., 1981, *Astronomy and Astrophysics*, 95, 105
- van der Kruit P., Jiménez-Vicente J., Kregel M., Freeman K., 2001, *Astronomy & Astrophysics*, 379, 374

9 APPENDIX- A

We will present the results pertaining to each galaxy constituting our sample superthin galaxies.

9.1 UGC7321

We describe the results obtained from dynamical modeling of UGC 7321 as constrained by stellar photometry in the *B*-band in addition to HI 21cm radio-synthesis observations. The central stellar dispersion $\sigma_{0s} = (10.2 \pm 0.6) \text{ kms}^{-1}$, which falls off exponentially with a scalelength of $(2.6 \pm 0.6) R_D$. In comparison, the central value of the vertical velocity dispersion of the stellar disc in the Milky Way [Lewis & Freeman \(1989\)](#) and the Andromeda or M31 ([Tamm et al. 2007](#)) is about $\sim 53 \text{ kms}^{-1}$. This is assuming that the stellar radial velocity dispersion falls off exponentially with a scale length of $2 R_D$ as is observed in the Galaxy, and also the ratio of the vertical to the radial stellar velocity dispersion is 0.5 at all radii, equal to its observed value in the solar neighbourhood ([Binney & Merrifield 2008](#)). This confirms that UGC7321 has an ultra-cold stellar disc with unusually low values of the vertical velocity dispersion of stars. The central value of HI dispersion $11.1 \pm 0.9 \text{ kms}^{-1}$ with $\alpha_{HI} = 0.2 \pm 0.1$ and $\beta_{HI} = -0.04 \pm 0.02$, thus indicating that the HI dispersion remains almost constant with R . We check the consistency of the multi-component model with the publicly-available stellar dynamical code AGAMA. Using the best-fitting value of the vertical stellar dispersion as obtained from the multi-component model as an input to AGAMA, we find that the scaleheight predicted by AGAMA complies with that from the multi-component model. Finally, we calculate multi-component disc dynamical stability parameter Q_{RW} as function of R . We find that the minimum value of Q_{RW} is 2.7 at about $5 R_D$, thus confirming that UGC 7321 is stable against the growth of axisymmetric

perturbations inspite of having an ultra-cold stellar disc. The central value of dispersion for the thin disc is $9.02 \pm 0.8 \text{ kms}^{-1}$, and it falls off exponentially with scale length $(4.6 \pm 0.7) R_{d2}$, where R_{d2} is the scale length of the thin disc. Interestingly, the vertical velocity dispersion profile of the thin disc of the $3.6 \mu\text{m}$ stellar component almost matches the profile from the *B*-band component within error bars. The central value for the thick disc is $24.7 \pm 0.9 \text{ kms}^{-1}$, falling off exponentially with disc scale length $(2.2 \pm 0.6) R_{d1}$, R_{d1} being the scale length of the thick disc. At small R , the density averaged vertical velocity dispersion is reflective of the cold, dense and compact thin disc. The central value of HI dispersion $11.2 \pm 0.8 \text{ kms}^{-1}$ with $\alpha_{HI} = -0.3 \pm 0.8$ and $\beta_{HI} = -0.04 \pm 0.02$, again indicating that the HI dispersion remains almost constant with R . We note that the vertical velocity dispersion profile of HI as obtained from two models using different tracers for the stellar disc are comparable. In Figure 4, we present the posterior probability distribution of the parameters of the multi-component model of the galactic disc of UGC7321 with the stellar component modelled by *B*-band [Left Panel] and $3.6\mu\text{m}$ photometry [Right Panel].

9.2 IC5249

Our calculations show that the central value of the stellar vertical velocity dispersion of the thick disc is $20.6 \pm 0.6 \text{ kms}^{-1}$, which falls off exponentially with scale length $(2.2 \pm 0.2) R_{d1}$. The same for the thin disc is found to be $9.3 \pm 0.4 \text{ kms}^{-1}$ with an exponential fall-off scale length of $(7.5 \pm 0.2) R_{d2}$. At $R > R_{d1}$, the density averaged vertical velocity dispersion converges to the value of the vertical velocity dispersion profile of the thick disc, which is hot, diffuse and extended. The central value of HI dispersion is $12.4 \pm 0.5 \text{ kms}^{-1}$ with $\alpha_{HI} = -0.9 \pm 0.1$ and $\beta_{HI} = -0.04 \pm 0.01$, thus indicating that the HI dispersion remains almost constant with R . Although the results from the two models for the thin disc are fairly comparable, the same does not seem to hold true for the thick disc, possibly because of its large scale height value. We find that the minimum value of Q_N is 1.7 at about $3 R_{d1}$, indicating that IC5249 may be on the borderline as far as dynamical stability of the stellar disc is concerned. In Figure 5, we present the posterior probability distribution of the parameters of the multi-component model of the galactic disc of IC5249 with the stellar component modelled by the $3.6\mu\text{m}$ photometry

9.3 FGC1540

Unlike our other sample galaxies, FGC1540 has two stellar discs in the optical. The central value of the vertical velocity dispersion of the thick disc is $36.9 \pm 1.1 \text{ kms}^{-1}$ and falls off with an exponential scale length of $3.7 \pm 0.4 R_{d1}$. The central dispersion for the thin disc is $13.1 \pm 1.2 \text{ kms}^{-1}$, the scale length of exponential fall-off being $3.3 \pm 0.4 R_{d2}$, where R_{d2} . The density averaged dispersion is reflective of the value of the thin disc component at all R . Due to the unavailability of the HI scale height data, we use a constant HI scale height of about 400 kpc at all radius (Kurapati, private communication) We find that the results for the thin disc are fairly comparable. However, as before, the results for the thick disc, which seem to be hotter than most of our sample galaxies, do not seem to be consistent with each other. We calculate Q_N as a function of R , indicating a minimum value of 1.9. The central vertical velocity dispersion of the thick disc is $16.2 \pm 0.9 \text{ kms}^{-1}$ and falls off exponentially with scale length $3.8 \pm 0.4 R_{d1}$. The same for the thin disc is $6.9 \pm 0.6 \text{ kms}^{-1}$, with a scale length of $12.1 \pm 0.2 R_{d2}$. The density averaged dispersion converges with the thick disc value at large R . We note that the vertical velocity dispersion profiles of the thin disc in the optical fairly band matches with the thick disc in the $3.6 \mu\text{m}$ band. However, as discussed earlier, disparity in their central surface density values possibly rules out the fact that they trace the same disc.

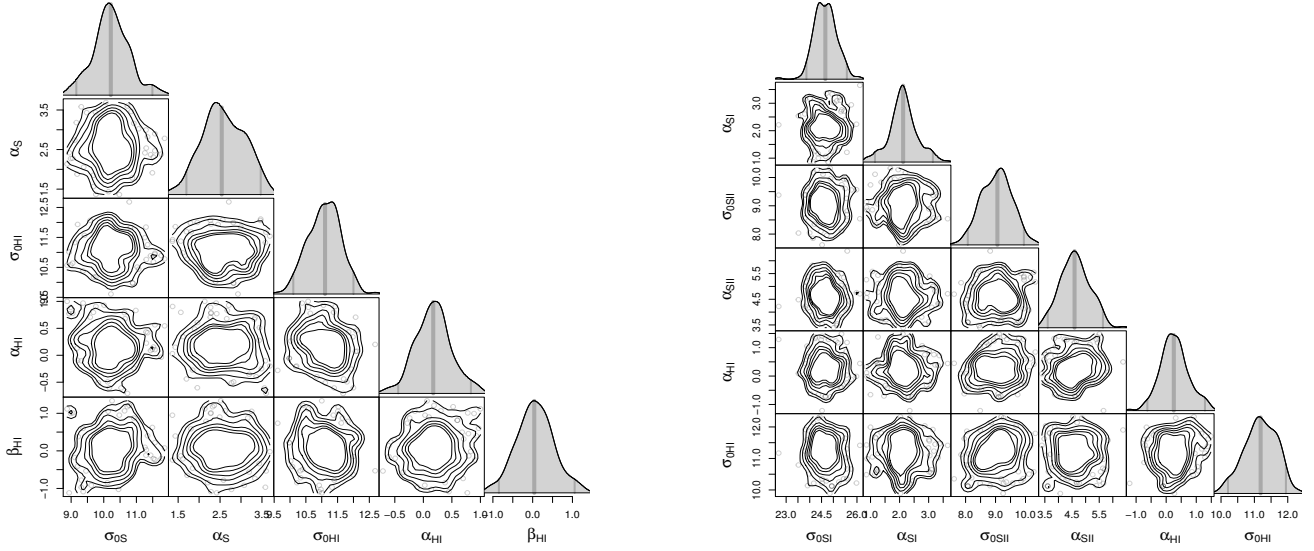


Figure 6. Posterior probability distribution and covariance plots of the parameters of the multi-component model of the galactic disc of UGC7321 with the stellar component modelled by *B*-band [Left Panel] and $3.6\mu\text{m}$ photometry [Right Panel]

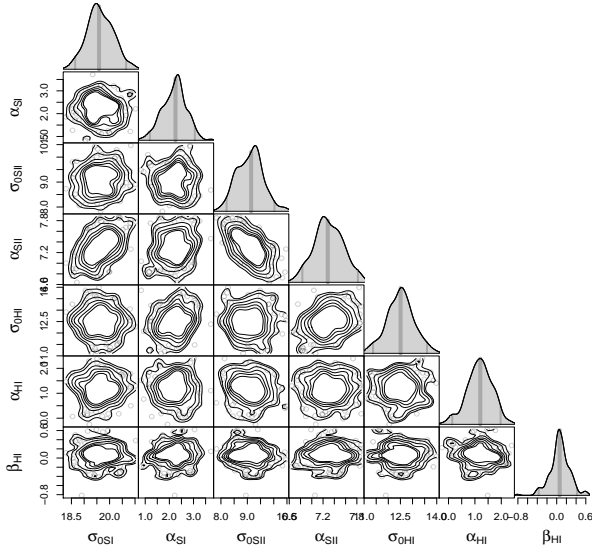


Figure 7. Posterior probability distribution and covariance plots of the parameters of the multi-component model of the galactic disc of IC2233 with the stellar component modelled by $3.6\mu\text{m}$ photometry

The minimum value of Q_N is 2.9, indicating the disc can resist the growth of axis-symmetric instabilities. In Figure 6, we present the posterior probability distribution of the parameters of the multi-component model of the galactic disc of FGC1540 in *i*-band [Left Panel] and $3.6\mu\text{m}$ photometry [Right Panel].

9.4 IC2233

The central velocity dispersion of IC2233 in *r*-band is $14.9 \pm 0.6 \text{ km s}^{-1}$ and a scalelength of exponential fall-off equal to 2.4 ± 0.4 . We have calculated the Q_N as function of R which has a minimum value of $Q_N \sim 2.2$, confirming the stability of the disc against growth of axis-symmetric instabilities. The central vertical velocity dispersion of the thick disc in $3.6\mu\text{m}$ is $15.9 \pm 0.5 \text{ km s}^{-1}$ and falls off exponentially with a scale length of $(2.2 \pm 0.4) R_{d1}$; the corresponding values for the thin disc are $3.9 \pm 0.2 \text{ km s}^{-1}$ and $(6.0 \pm 0.2) R_{d2}$. The density averaged vertical velocity dispersion does not seem to reflect any component in particular, but remains constant at 6 km s^{-1} at all R . The scaleheight from two component model and AGAMA seem to match fairly well both for the thin and thick disc cases. The multi-component stability parameter Q_N in $3.6 \mu\text{m}$ has a minimum value of is 5.7, which implies that the disc is highly stable against axis-symmetric instabilities. In Figure 7, we present the posterior probability distribution and covariance plots of the parameters of the multi-component model of the galactic disc of IC2233 with the stellar component modelled by *r*-band [Left Panel] and $3.6\mu\text{m}$ photometry [Right Panel]

9.5 UGC00711

The central vertical velocity dispersion in *B*-band is $18.4 \pm 0.9 \text{ km s}^{-1}$, and falls off exponentially with a scale length of $(3.2 \pm 0.4) R_{d1}$ where R_{d1} is the exponential scale length of the optical disk. We have calculated Q_N as a function of R , we find that the minimum value is 4.5, indicating the disc is highly stable. The central velocity dispersion in $3.6\mu\text{m}$ is $23.8 \pm 1.5 \text{ km s}^{-1}$, the dispersion falls off exponentially with scalelength $(2.4 \pm 0.3) R_{d1}$. The minimum value of Q_N is 4.3. We note that the vertical velocity dispersion as well as the disk dynamical stability profiles of the optical and the $3.6 \mu\text{m}$ disc of UGC00711 match well with each other, possibly confirming that they represent one and the same disc. In Figure 8, we present the posterior probability distribution and covariance plots of the parameters of the multi-component model of

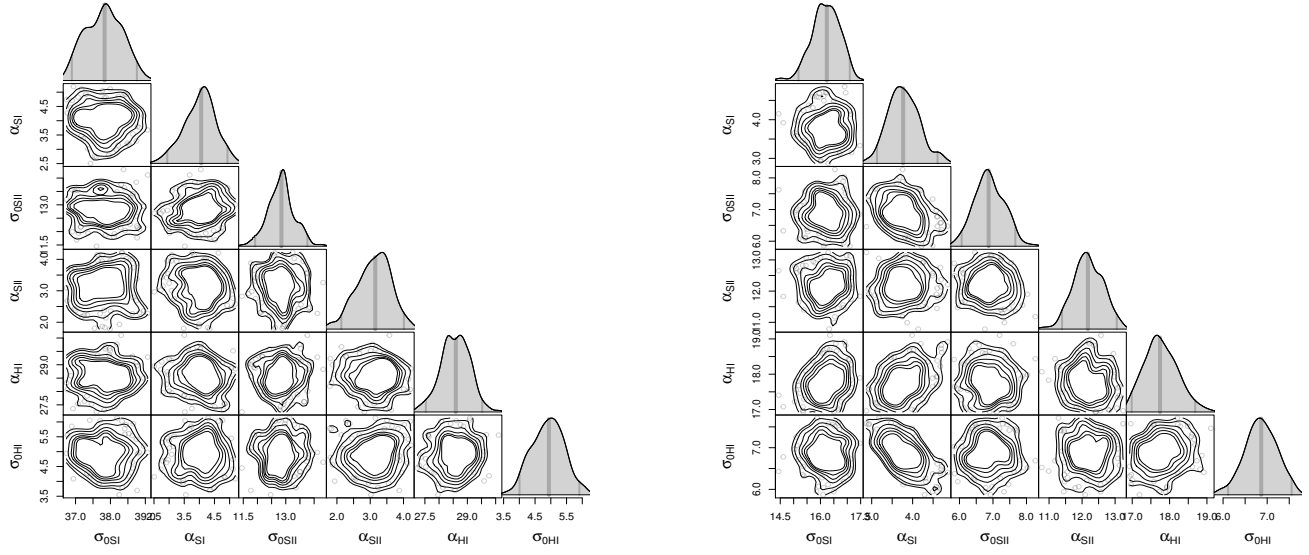


Figure 8. Posterior probability distribution and covariance plots of the parameters of the multi-component model of the galactic disc of FGC1540 with the stellar component modelled by *i*-band [Left Panel] and $3.6\mu\text{m}$ photometry [Right Panel]

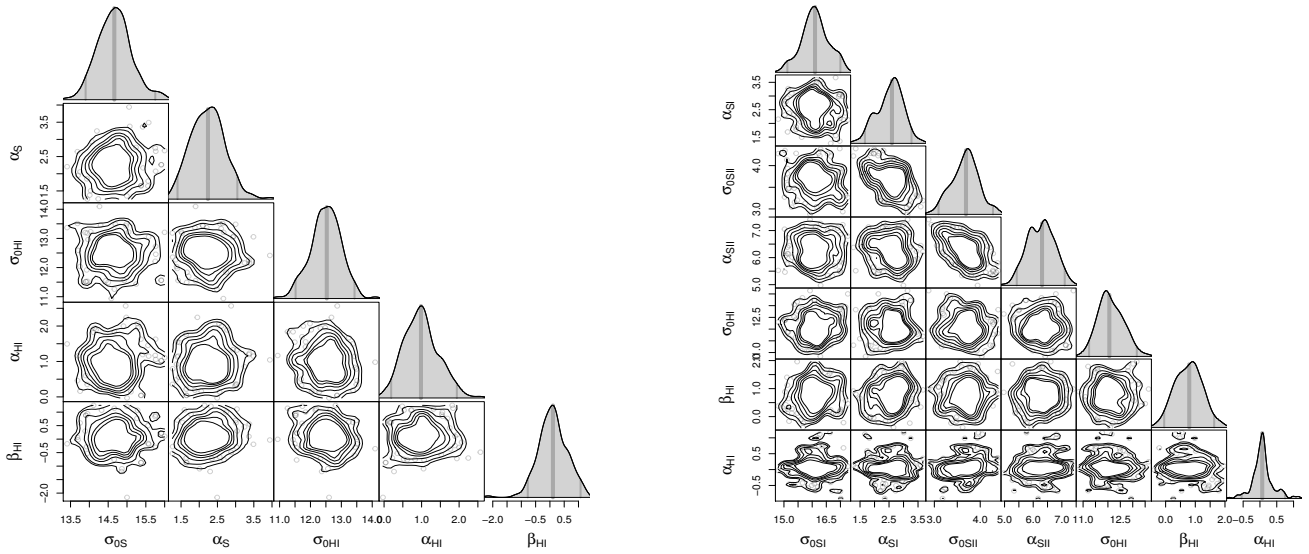


Figure 9. Posterior probability distribution and covariance plots of the parameters of the multi-component model of the galactic disc of IC2233 with the stellar component modelled by *r*-band [Left Panel] and $3.6\mu\text{m}$ photometry [Right Panel]

the galactic disc of UGC711 with the stellar component modelled by *r*-band [Left Panel] and $3.6\mu\text{m}$ photometry [Right Panel]

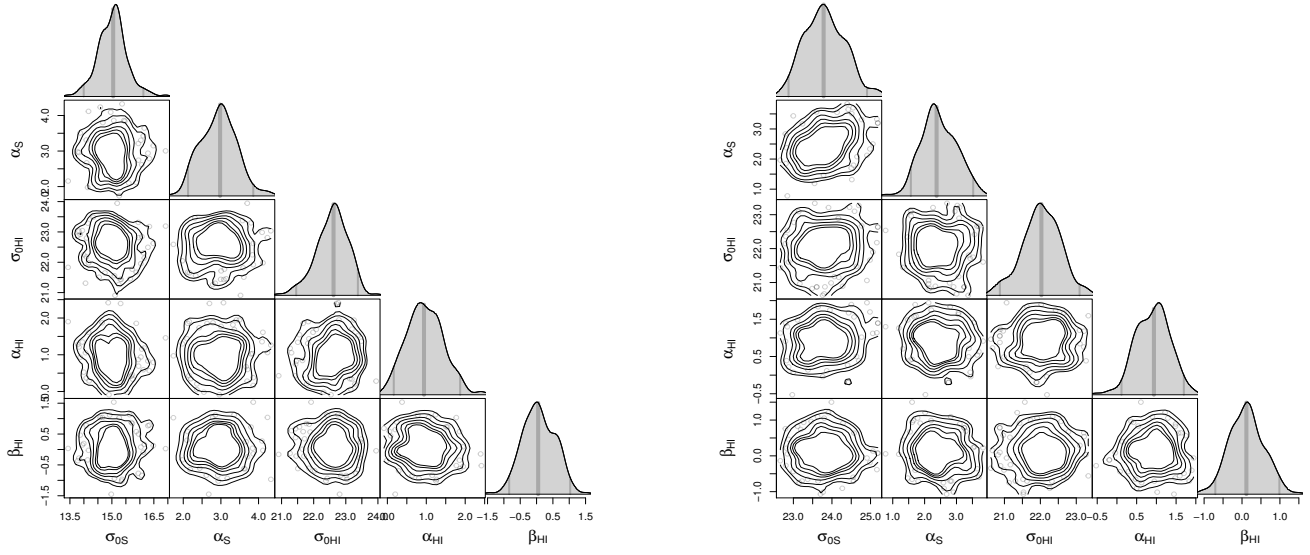


Figure 10. Posterior probability distribution and covariance plots of the parameters of the multi-component model of the galactic disc of UGC00711 with the stellar component modelled by *B*-band [Left Panel] and $3.6\mu\text{m}$ photometry [Right Panel]